

Multimodal Active Measurement for Human Mesh Recovery in Close Proximity

Takahiro Maeda^{1,*}, Keisuke Takeshita², and Kazuhito Tanaka²

Abstract—For safe and sophisticated physical human-robot interactions (pHRI), a robot needs to estimate the accurate body pose or mesh of the target person. However, in these pHRI scenarios, the robot cannot fully observe the target person’s body with equipped cameras because the target person is usually close to the robot. This leads to severe truncation and occlusions, and results in poor accuracy of human pose estimation. For better accuracy of human pose estimation or mesh recovery on this limited information from cameras, we propose an active measurement and sensor fusion framework of the equipped cameras and other sensors such as touch sensors and 2D LiDAR. These touch and LiDAR sensing are obtained attendantly through pHRI without additional costs. These sensor measurements are sparse but reliable and informative cues for human mesh recovery. In our active measurement process, camera viewpoints and sensor placements are optimized based on the uncertainty of the estimated pose, which is closely related to the truncated or occluded areas. In our sensor fusion process, we fuse the sensor measurements to the camera-based estimated pose by minimizing the distance between the estimated mesh and measured positions. Our method is agnostic to robot configurations. Experiments were conducted using the Toyota Human Support Robot, which has a camera, 2D LiDAR, and a touch sensor on the robot arm. Our proposed method demonstrated the superiority in the human pose estimation accuracy on the quantitative comparison. Furthermore, our proposed method reliably estimated the pose of the target person in practical settings such as target people occluded by a blanket and standing aid with the robot arm.

I. INTRODUCTION

3D human pose estimation or human mesh recovery is the key technique for assistive robots to physically interact with humans safely and appropriately. For example, to achieve care robots helping elderly or physically challenged people to stand up easily and safely, robots need to utilize pose estimation to decide where to support with their arms and even detect unstable posture and falling based on the estimated pose. However, robots in pHRI scenarios usually cannot fully observe the human body with equipped cameras because occlusions and image truncations happen at a very close range. Human pose estimation methods perform poorly with these settings due to limited information, as shown in the upper part of Fig. 1.

However, humans still have good capability to estimate the poses of other humans in very close range by actively moving their heads and eyes to a more informative viewpoint

*Work done during the internship at Frontier Research Center, Toyota Motor Corporation

¹Department of Advanced Science and Technology, Toyota Technological Institute, Nagoya, Aichi, Japan. sd21601@toyota-ti.ac.jp

²R-Frontier Division, Frontier Research Center, Toyota Motor Corporation, Toyota, Aichi, Japan.

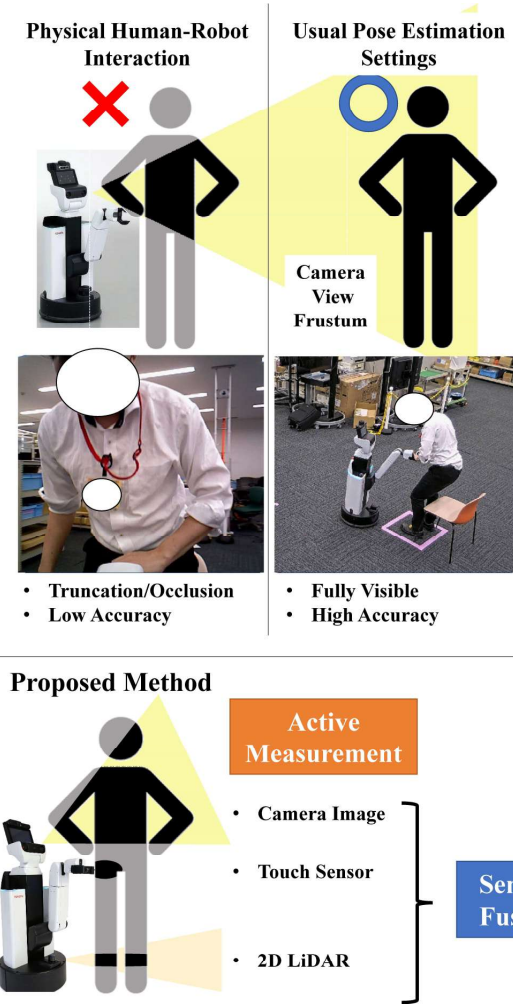


Fig. 1: Problem of previous human pose estimation methods in pHRI scenarios and our proposed method.

and using multimodal cues such as tactile and temperature information from their skin. Physically interactive robots should perform the same by actively operating their joints and wheels/legs and incorporating multimodal sensor inputs for better accuracy, as shown in the bottom part of Fig. 1.

To achieve this, we propose a new human mesh recovery method for physically interactive robots in close proximity. Our proposed framework has two components: *active measurement* and *sensor fusion*. In the *active measurement*, the robot viewpoint and sensor positions are optimized one by one to cover the whole body and leave less uncertain areas. In this optimization, we use the positional variance

of estimated poses as the estimation uncertainty, which is closely related to the unobserved areas by truncations and occlusions. Camera viewpoints are optimized to cover the uncertainty-weighted largest body surfaces. Other sensor placements are optimized to measure the most uncertain area within the feasible robot poses. In the *sensor fusion* part, estimation from cameras is improved by aligning poses consistent with sensor measurements using an optimization algorithm. Specifically, we minimize the distance between the estimated mesh to the sensor measurement positions. Our contributions are as follows,

- We propose the active measurement framework for human mesh recovery using multimodal sensors. Our method optimizes the camera viewpoint and sensor placement to cover the whole body and leave less uncertain areas.
- Our sensor fusion method improves estimated poses by incorporating multimodal measurements such as touch/force/torque or LiDAR sensors. The estimated poses are improved by minimizing the distance between the estimated mesh and sensor measurements.
- We quantitatively show the accuracy improvement by the experiments with the Toyota Human Support Robot. Furthermore, we also show the effectiveness of our method in practical scenarios such as the target person occluded with a blanket and standing aid with the robot arm.

II. RELATED WORK

There has been significant progress in human pose estimation from RGB images, starting from 2D [5], [39], [45], [46], [51] to 3D [12], [33], [42], [53], [54] and mesh recovery [4], [9], [11], [21], [26], [29], [52]. However, most existing methods assume input images are taken from enough distance without occlusions and view-dependent truncations. Therefore, in physical human-robot interaction scenarios, the following three techniques should be considered to deal with occlusions and truncations that happen in close proximity.

Pose estimation robust to occlusions and view-dependent truncations. Some methods utilize attention mechanisms to focus on visible areas to ensure the robustness to occlusions [14], [22], [25], [59]. However, it is difficult to adequately train attention mechanisms due to the scarcity of occluded data. Data augmentation [8], [35], [38], [48] is an easy way for simulating these occluded or truncated data, but cannot fully capture the complexity of real-world occlusions and truncations. Besides the previous methods on annotated pose-image pair, we can create pose prior [7] as Generative Adversarial Networks [13] trained on large pose datasets such as AMASS [32]. It can ensure that the output pose is biologically plausible by discriminating poses outside the distribution of the AMASS dataset.

The methods above are applied to regression models. However, it is inherently inappropriate to choose the deterministic regression models for the highly ill-posed problem such as human pose estimation on severely truncated and occluded

images. Some methods use probabilistic models to regress multiple pose hypotheses [3], [18], [27], [28], [44].

Although these methods above can improve estimated poses on ambiguous images, their estimations are just guessing truncated or occluded body parts. In physical human-robot interaction scenarios, robots can move to viewpoints with fewer occlusions and truncations.

Pose estimation with active measurements. The quality of the viewpoints is often expressed as estimated error metrics or uncertainty of human pose estimation [6], [23]. Specifically, Kiciroglu *et al.* [23] performs quadratic approximation to the error landscape on each possible viewpoint and treats the approximated variance as the uncertainty. This method assumes no truncations and thus fails to model the complex error landscape with severe truncations. In contrast, Arzati *et al.* [2] optimizes the flight drone viewpoints by deep reinforcement learning for dermatology applications. DQN [34] is trained in simulation environments based on the reward related to the accuracy of pose estimation. This reward considers only visible body parts and ignores the pose estimation accuracy of the truncated body part by camera views. In addition to this active measurement, robots usually have multimodal sensors other than cameras. They may improve the pose estimation accuracy by complementing limited information from camera observations.

Pose estimation with multimodal data. Depth and point cloud sensors are the most common modality other than cameras in human pose estimation [19], [20], [30], [43], [47], [58] Although they can alleviate the depth ambiguity problem and provide accurate estimations, they have minimum depth distance for measurements, which is inappropriate for human pose estimation in close range. Wearable Inertia Measurement Units (IMUs) can track the position and orientation of specific body parts and also help human pose estimation [16], [17], [40], [41], [55]. However, it is inconvenient to wear IMUs to be assisted by robots. Furthermore, wearing IMUs for a long time causes drifting and results in less accurate measurements. Zhao *et al.* [56], [57] use the unique modality, radio frequency signals, to estimate human poses. Although we can estimate the pose of people behind a wall thanks to the characteristics of radio frequency signals, their spatial resolution is low. In this paper, we focus on the cues attendantly obtained through pHRI without additional costs such as touch sensors. The other possible options are discussed in Sec. V.

III. PROPOSED METHOD

Our proposed method is described in this section. The overview is shown in Fig. 2.

A. Problem Formulation

The objective is to estimate human 3D joint positions $J \in \mathbb{R}^{3 \times N_{joint}}$, where N_{joint} is the number of joints. The available information is multimodal measurements including a camera image $I(R_c, t_c)$ containing a person and other K sensor placements $(R_1, t_1), \dots, (R_K, t_K)$ such as 2D LiDAR and a touch sensor measuring the person's body

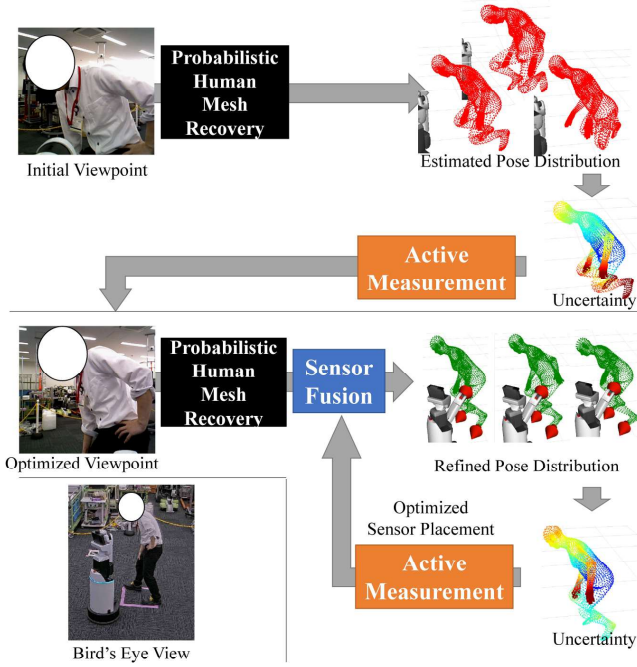


Fig. 2: Overview of our proposed method.

surface, where R_c and t_c are the camera orientation and translation, and R_k and t_k are the k -th sensor orientation and translation accordingly. All sensor positions including a camera are optimized by the active measurement framework for better accuracy of human pose estimation.

B. SMPL Model

We use Skinned Multi-person Linear Body (SMPL [31], [36]) as an intermediate representation of human poses. SMPL is a neural network $V_{\text{local}} = \mathcal{M}(\theta, \beta)$ that map a set of pose parameters θ and body parameters β to a human body mesh without a global pose $V_{\text{local}} \in \mathbb{R}^{3 \times 6890}$ with 6890 vertices. The pose parameters θ contain the axis-angle representation of each body joint rotation. The shape parameters β control the body height, weights, and limb length. We can obtain the human body mesh on the world coordinates V using a global pose (R_p, t_p) as $V = R_p V_{\text{local}} + t_p$. Global body joint positions J are also regressed by a linear weight W as $J = R_p W V_{\text{local}} + t_p$. We can induce the biological constraints by explicitly using these body models as an intermediate representation. Moreover, We use the generated mesh vertices V to fuse the other modality sensor measurements into the estimated pose, as explained in Sec. III-E.

C. Probabilistic Human Mesh Recovery

Human mesh recovery is a task to estimate the set of pose parameters θ , body parameters β , and the global pose (R_p, t_p) , which defines the human mesh vertices V and eventual joint positions J , given the camera image I containing a person. We use a probabilistic approach to utilize the estimation uncertainty. Conditional probability distribution $p(\theta, \beta | I)$ is obtained by the probabilistic human

mesh recovery. Given this distribution, we can also *regress* the pose via maximum likelihood as follows.

$$V_{\text{ML}} = R_p \mathcal{M}(\theta_{\text{ML}}, \beta_{\text{ML}}) + t_p \quad (1)$$

$$J_{\text{ML}} = R_p W \mathcal{M}(\theta_{\text{ML}}, \beta_{\text{ML}}) + t_p \quad (2)$$

$$\text{where, } \theta_{\text{ML}}, \beta_{\text{ML}} = \arg \max_{\theta, \beta} p(\theta, \beta | I) \quad (3)$$

Furthermore, the uncertainty of the estimated pose is calculated as the positional variance $\sigma_{\text{mesh}} \in \mathbb{R}^{6890}$ of each mesh vertex as follows,

$$\sigma_{\text{mesh}} = \mathbb{E}_{(\theta, \beta) \sim p(\theta, \beta | I)} [\mathcal{M}(\theta, \beta)] \quad (4)$$

This uncertainty is strongly related to the occluded or truncated area and can determine the effective camera and sensor positions via our active measurement framework.

D. Active Measurement

Each sensor placements $(R_c, t_c), (R_1, t_1), \dots, (R_K, t_K)$ is optimized based on the uncertainty of the estimated pose σ_{mesh} . We optimize each sensor placement one by one. Specifically, after the optimization of one sensor, we update the estimated poses and corresponding uncertainty σ_{mesh} based on the new optimized sensor measurement as described in Sec. III-E.

For the equipped camera, viewpoint (R_c, t_c) is optimized to cover the largest body surface within the camera image. We consider the camera projection function π that projects a 3D position to the camera coordinates and checks the self-occlusion as the following,

$$x_i, y_i, \text{Occ}_i = \pi(v_i; V, R_c, t_c) \quad (5)$$

, where x_i, y_i are the projected position on the camera coordinate $x_i \in [0, W], y_i \in [0, H]$. Occ denotes the boolean for occluded or not as $\text{Occ}_i \in \{0, 1\}$. v_i is a 3d position of i -th vertex from the mesh vertices V . Each camera viewpoint is evaluated based on the weighted mesh coverage as follows,

$$R_c^*, t_c^* = \arg \max_{R_c, t_c} \sum_{v_i \in V_{\text{ML}}} \sigma_{\text{mesh}, i} (1 - \text{Occ}_i) \quad (6)$$

This allows us to optimize the camera viewpoint to cover more body surfaces with higher uncertainty, which leads to less occluded and truncated areas.

For other sensors that measure the body surface, placements $(R_1, t_1), \dots, (R_K, t_K)$ are optimized one by one to complement the limited information from the optimized viewpoint. Specifically, we exclude the kinematically impossible placements by solving inverse kinematics (IK) and select the most uncertain mesh vertex to measure as follows,

$$R_k, \mathbf{t}_k, \text{Suc}_i = \text{IK} \left(\mathbf{v}_i; (R_c^*, \mathbf{t}_c^*), (R_1^*, \mathbf{t}_1^*), \dots, (R_{k-1}^*, \mathbf{t}_{k-1}^*) \right) \quad (7)$$

$$i^* = \arg \max_{i \in [0, 6890]} \sigma_{\text{mesh}, i} \times \text{Suc}_i \quad (8)$$

$$R_k^*, \mathbf{t}_k^*, 1 = \text{IK} \left(\mathbf{v}_{i^*}; (R_c^*, \mathbf{t}_c^*), (R_1^*, \mathbf{t}_1^*), \dots, (R_{k-1}^*, \mathbf{t}_{k-1}^*) \right) \quad (9)$$

, where IK is the inverse kinematics function that takes a 3D position \mathbf{v}_i of i -th mesh vertex and already optimized sensor placements as input, and outputs the target sensor placement R_k, \mathbf{t}_k which sensing the 3D position \mathbf{v}_i and Suc_i denotes the boolean for whether there is a feasible robot pose satisfying the all optimized sensor placement requirements. If the target sensor has limited freedom for placement due to the robot's task such as supporting the human body, we simply perform the optimization within the allowed joint range.

We can easily extend the active measurement framework above to sense the multiple mesh vertices using the pressure sensor array. After the sensor placement optimization, we fuse the multimodal information to improve the pose estimation as described in the next subsection.

E. Sensor Fusion

Our sensor fusion improves estimated poses by aligning the estimated mesh V consistent with body surface measurements from currently optimized k sensors $\mathbf{m}_1, \dots, \mathbf{m}_k$. The sensor fusion has two stages; global position offset and local pose optimization.

First, we offset the global position \mathbf{t}_p because camera-based estimated poses contain depth ambiguity due to an unknown person's height and inaccurate camera intrinsics. The offset is the mean vector between the measurements $\mathbf{m}_1, \dots, \mathbf{m}_k$ to the nearest mesh vertex $\mathbf{w}_1, \dots, \mathbf{w}_k$ as follows,

$$\mathbf{t}_{\text{offset}} = \mathbb{E}_{(\theta, \beta) \sim p(\theta, \beta | I)} \left[\frac{1}{k} \sum_{k'=1}^k \mathbf{w}_{k'} - \mathbf{m}_{k'} \right] \quad (10)$$

$$\mathbf{w}_k = \arg \min_{\mathbf{v}_i} \|\mathbf{v}_i - \mathbf{m}_k\| \quad (11)$$

After calculating offset, we optimize the pose parameter θ by minimizing the distance between the body surface and the sensor measurements via backpropagation as follows,

$$\theta^* = \arg \min_{\theta} L \quad (12)$$

$$L = \frac{1}{k} \sum_{k'=1}^k \|\mathbf{w}_{k'} - \mathbf{m}_{k'} - \mathbf{t}_{\text{offset}}\| \quad (13)$$

Using each optimized pose parameters θ^* , we update the positional variance σ_{mesh} and optimize the next sensor placement $R_{k+1}, \mathbf{t}_{k+1}$ by repeating the process iteratively. The updated positional variance σ'_{mesh} is expected to be small around the sensor measurements thanks to aligning via

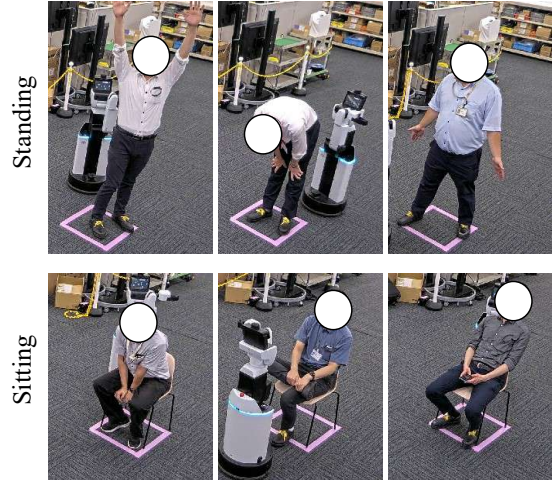


Fig. 3: Evaluated poses on two pose groups: standing and sitting.

optimization. Therefore, it is possible to select the different uncertain vertex by using σ'_{mesh} . The maximum-likelihood estimated pose with this sensor fusion θ_{ML}^* is used for evaluation.

IV. EXPERIMENTS

A. Experimental Setup

Quantitative experiments were conducted to show the effectiveness of our proposed method. We also conducted experiments on practical scenarios of a person occluded by a blanket and standing aid with the robot arm. Toyota Human Support Robot [15], [49], [50] was used in the experiments. The HSR has RGB cameras, a force sensor in the wrist joint, and 2D LiDAR. The RGB camera has 5 degrees of freedom by the omnidirectional moving base, the lifting joint, and the pan/tilt joint. The force sensor has 3 degrees of freedom by the yaw rotation of the omnidirectional moving base and the robot arm. The 2D LiDAR has 3 degrees of freedom by the omnidirectional moving base. We applied a leg detection filter to the 2D LiDAR measurements to exclude the walls and other objects. We used ProHMR [27] as the off-the-shelf probabilistic human mesh recovery. However, model weights were trained from scratch with a focal length of 2200 to deal with the changing focal length between training and test [24]. For the quantitative evaluation, the ground truth poses are measured by markerless human motion capture EasyMocap [1]. EasyMocap utilizes multiple calibrated RGB environmental cameras to satisfy enough accuracy to create the human motion dataset ZJU-Mocap [10], [37]. We used six environmental cameras and calibrated them with the chessboard pattern.

B. Quantitative Results

We evaluated the accuracy of human pose estimation on ten subjects, eight initial viewpoints, and two pose groups. Therefore, 160 poses are evaluated in total. Human Support Robot estimates the subject pose with our active measurement and sensor fusion from a constant 0.7-meter distance to

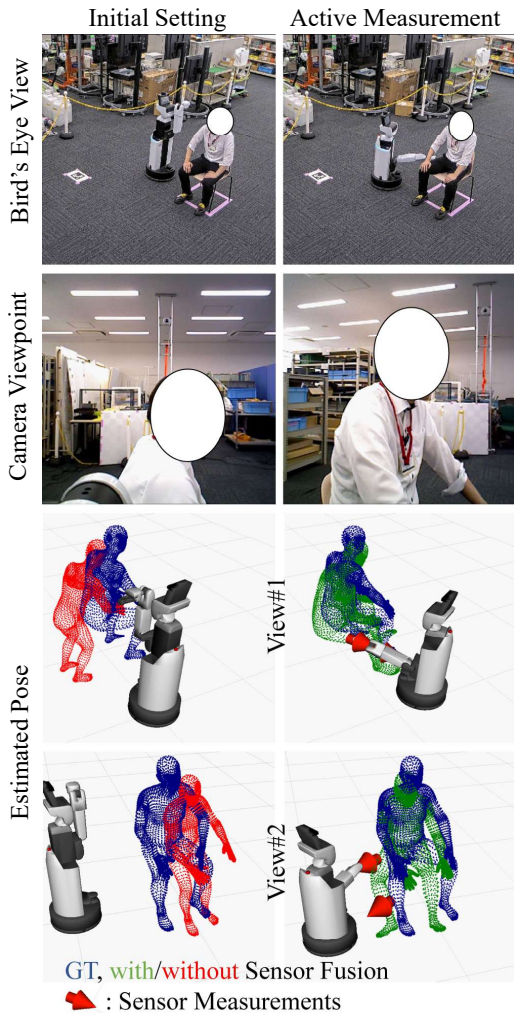


Fig. 4: Visualization of quantitative evaluation.

the subject. The viewpoint is initialized to view the subject from one of eight directions with 45-degree intervals. At the viewpoint initializations, the subjects are directed to take different poses from one of two pose groups: standing and sitting as shown in Fig. 3. The subjects are 163-187 centimeter-tall adults with around 60-110 kilogram weights.

We report the mean Euclidean distance per joint, in Tab. I and Tab. II. The proposed method achieved the lowest pose estimation error averaged on all joints in both two pose groups. Our camera active measurement can greatly decrease the estimation error by around 30 percent. Sensor fusion of touch sensors can reduce the error of all joints by sensing the whole body relatively freely and complementing limited information from the camera. In contrast, 2D LiDAR mainly improves the estimation of leg poses by sensing the occupation of the area near the floor. 2D LiDAR can reduce the estimation error of ankle joints to half in the standing pose group. The estimated poses are visualized in Fig. 4. The estimated poses are improved by covering more body surface and touching the thigh with the robot arm.

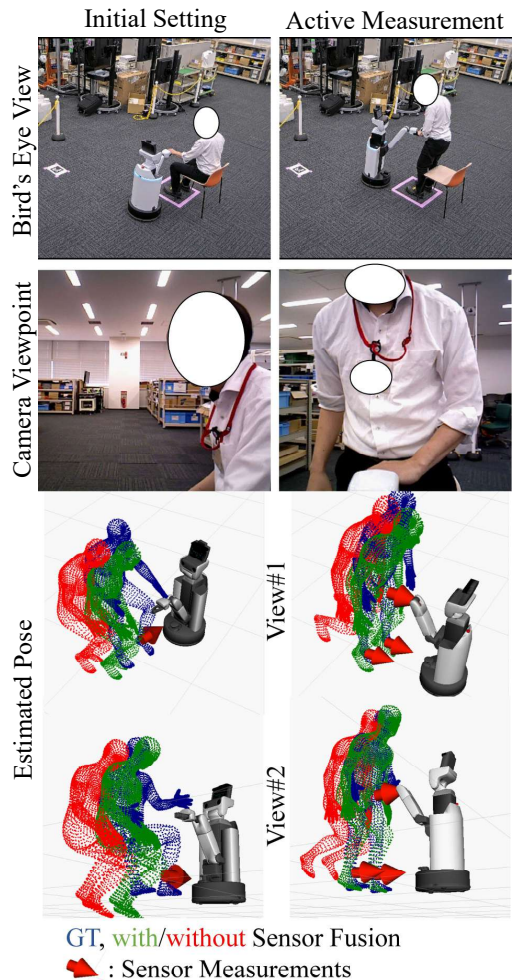


Fig. 5: Visualization of the standing aid scenario.

C. Estimation Accuracy on Practical Scenarios

The quantitative evaluations prove the effectiveness of our method with no restriction on camera and sensor placements. However, the practical pHRI scenarios have several restrictions on them depending on the target task.

Standing Aid Scenario. When assistive robots support human bodies or hand something to a person, robot arms need to reach certain positions. We mocked this situation and experimented with the standing aid scenario. The Human Support Robot optimizes the camera viewpoint while its end effector follows a certain lifting trajectory. The estimated poses are visualized in Fig. 5. The proposed method estimates the poses closer to the ground truth with the restriction on the touch sensor. The viewpoint is moved from the side low view to the front high view to cover the larger body surface and follow the target person standing up. The leg positions are mainly improved by the sensor fusion.

Occluded by a Blanket Scenario. Active measurement on camera viewpoints may not be effective in several cases. For example, the target person is under a comforter on a bed or blanket while sitting. Furthermore, wearing loose-fitting clothes such as dresses, hospital patient gowns, and kimonos

TABLE I: Quantitative results on standing poses.

Active Measurement & Sensor Fusion			Euclidean Distance Error [mm]						
Camera	Touch Sensor	2D LiDAR	Head	Pelvis	R Wrist	L Wrist	R Ankle	L Ankle	All Joints
✓			400.4	370.7	437.3	409.1	533.4	547.5	418.1
✓	✓		210.6	224.4	274.0	275.4	428.7	442.5	266.5
✓		✓	210.2	201.5	256.6	264.3	387.1	400.8	249.8
✓	✓	✓	276.5	215.9	288.2	298.8	210.7	210.5	243.0
			269.1	203.9	275.8	287.6	202.8	215.8	235.9

TABLE II: Quantitative results on sitting poses.

Active Measurement & Sensor Fusion			Euclidean Distance Error [mm]						
Camera	Touch Sensor	2D LiDAR	Head	Pelvis	R Wrist	L Wrist	R Ankle	L Ankle	All Joints
✓			452.7	514.0	515.2	510.6	791.3	759.5	572.4
✓	✓		206.3	273.9	322.1	298.5	539.1	534.4	322.9
✓		✓	219.3	212.6	293.0	264.1	446.9	449.9	284.2
✓	✓	✓	206.1	199.1	267.6	254.2	442.9	415.4	274.9
			210.3	192.7	267.1	249.5	419.4	405.8	270.0



Fig. 6: Visualization of the scenario of the target person with a blanket.

also affects viewpoint optimization. However, the proposed method can still estimate the accurate pose thanks to the multimodality of inputs because touch sensors are robust to these occlusions and reliably obtain the body surface information. We experimented with a scenario where the target person was occluded by a blanket. Human Support Robot estimates the poses of the target person with a blanket on the person’s lower body. The touch sensor placement is optimized while the camera viewpoint is fixed. The 2D LiDAR measurements were not utilized because the leg was not detected due to the broad blanket surface. The estimated poses are visualized in Fig. 6. The proposed method estimates the poses closer to the ground truth in spite of a fixed camera viewpoint and sparse touch measurement.

V. DISCUSSION

In this section, we discuss the validity of our experimental setting with a single camera and additional sensors.

Multiple Calibrated Environmental cameras may estimate accurate poses as EasyMocap [1] and ZJU-Mocap dataset [10], [37]. However, environmental cameras face serious privacy problems. Usually, no environmental camera is allowed in restrooms because of privacy violations to others despite the need for standing aid of elderly or physically challenged people. Furthermore, environmental cameras are not available outside the buildings. It is straightforward to utilize only a camera mounted to the robot body.

Multiple cameras on multiple robot arms may also estimate accurate poses by triangulation and more visible area. However, multiple cameras on multiple robot arms face

complicated kinematic constraints. In physical human-robot interaction scenarios, there are already several robot arms used for interactions such as handing objects and supporting a human body. Thus, it is difficult to move multiple cameras with arms to informative viewpoints under the constraints of a stable center of mass and free from self-collisions. Although we didn’t conduct experiments with multiple cameras for the above reasons, one can easily replace the probabilistic human mesh recovery model to accept the multiple images of the target person.

VI. CONCLUSION

In this paper, we proposed a multimodal active measurement framework for human mesh recovery that can estimate accurate human poses even in close proximity by using additional sensors such as tactile sensors. Experimental results demonstrated that our method achieved higher accuracy than methods without active measurement or additional sensor inputs even with severely truncated camera images.

Our proposed method has one limitation: slow inference. Our method takes 0.5 seconds to estimate poses due to the optimization process in the sensor fusion. We can achieve faster inference by replacing the learning-free optimization with supervised learning-based regression. In addition to this, we can incorporate temporal information or a previously estimated pose to skip the several processes in our proposed method. Our future work is achieving higher accuracy by using other sensors such as a pressure sensor array, proximity sensors, and thermometers.

REFERENCES

- [1] Easymocap - make human motion capture easier. Github, 2021.
- [2] Mojtaba Ahangar Arzati and Siamak Arzanpour. Viewpoint selection for dermdrone using deep reinforcement learning. In *IEEE International Conference on Control, Automation and Systems, ICCAS 2021*.
- [3] Benjamin Biggs, David Novotný, Sébastien Ehrhardt, Hanbyul Joo, Benjamin Graham, and Andrea Vedaldi. 3d multi-bodies: Fitting sets of plausible 3d human models to ambiguous image data. In *Annual Conference on Neural Information Processing Systems, NeurIPS 2020*.
- [4] Federica Bogo, Angjoo Kanazawa, Christoph Lassner, Peter V. Gehler, Javier Romero, and Michael J. Black. Keep it SMPL: automatic estimation of 3d human pose and shape from a single image. In *European Conference on Computer Vision, ECCV 2016*.
- [5] Zhe Cao, Tomas Simon, Shih-En Wei, and Yaser Sheikh. Realtime multi-person 2d pose estimation using part affinity fields. In *IEEE Conference on Computer Vision and Pattern Recognition, CVPR 2017*.
- [6] Kai-Chi Chan, Cheng-Kok Koh, and C. S. George Lee. Selecting best viewpoint for human-pose estimation. In *IEEE International Conference on Robotics and Automation, ICRA 2014*.
- [7] Yu Chen, Chunhua Shen, Xiu-Shen Wei, Lingqiao Liu, and Jian Yang. Adversarial posenet: A structure-aware convolutional network for human pose estimation. In *IEEE International Conference on Computer Vision, ICCV 2017*.
- [8] Yu Cheng, Bo Yang, Bo Wang, and Robby T. Tan. 3d human pose estimation using spatio-temporal networks with explicit occlusion training. In *The Thirty-Fourth AAAI Conference on Artificial Intelligence, AAAI 2020*.
- [9] Hongsuk Choi, Gyeongsik Moon, and Kyoung Mu Lee. Pose2mesh: Graph convolutional network for 3d human pose and mesh recovery from a 2d human pose. In *European Conference on Computer Vision, ECCV 2020*.
- [10] Qi Fang, Qing Shuai, Junting Dong, Hujun Bao, and Xiaowei Zhou. Reconstructing 3d human pose by watching humans in the mirror. In *IEEE Conference on Computer Vision and Pattern Recognition, CVPR 2021*.
- [11] Georgios Georgakis, Ren Li, Srikrishna Karanam, Terrence Chen, Jana Kosecká, and Ziyang Wu. Hierarchical kinematic human mesh recovery. In *European Conference on Computer Vision, ECCV 2020*.
- [12] Mohsen Gholami, Bastian Wandt, Helge Rhodin, Rabab Ward, and Z. Jane Wang. Adaptpose: Cross-dataset adaptation for 3d human pose estimation by learnable motion generation. In *IEEE/CVF Conference on Computer Vision and Pattern Recognition, CVPR 2022*.
- [13] Ian J. Goodfellow, Jean Pouget-Abadie, Mehdi Mirza, Bing Xu, David Warde-Farley, Sherjil Ozair, Aaron C. Courville, and Yoshua Bengio. Generative adversarial nets. In *Annual Conference on Neural Information Processing Systems, NeurIPS 2014*.
- [14] Renshu Gu, Gaoang Wang, and Jenq-Neng Hwang. Exploring severe occlusion: Multi-person 3d pose estimation with gated convolution. In *25th International Conference on Pattern Recognition, ICPR 2020*.
- [15] Kunimatsu Hashimoto, Fuminori Saito, Takashi Yamamoto, and Koichi Ikeda. A field study of the human support robot in the home environment. In *IEEE Workshop on Advanced Robotics and its Social Impacts, ARSO 2013*.
- [16] Fuyang Huang, Ailing Zeng, Minhao Liu, Qiuxia Lai, and Qiang Xu. Deepfuse: An imu-aware network for real-time 3d human pose estimation from multi-view image. In *IEEE Winter Conference on Applications of Computer Vision, WACV 2020*.
- [17] Yinghao Huang, Manuel Kaufmann, Emre Aksan, Michael J. Black, Otmar Hilliges, and Gerard Pons-Moll. Deep inertial poser: learning to reconstruct human pose from sparse inertial measurements in real time. *ACM Trans. Graph.*, 37(6):185, 2018.
- [18] Ehsan Jahangiri and Alan L. Yuille. Generating multiple diverse hypotheses for human 3d pose consistent with 2d joint detections. In *IEEE International Conference on Computer Vision Workshops, ICCVW 2017*.
- [19] Haiyong Jiang, Jianfei Cai, and Jianmin Zheng. Skeleton-aware 3d human shape reconstruction from point clouds. In *IEEE/CVF International Conference on Computer Vision, ICCV 2019*.
- [20] Abdolrahim Kadkhodamohammadi, Afshin Gangi, Michel de Mathelin, and Nicolas Padoy. A multi-view RGB-D approach for human pose estimation in operating rooms. In *IEEE Winter Conference on Applications of Computer Vision, WACV 2017*.
- [21] Angjoo Kanazawa, Michael J. Black, David W. Jacobs, and Jitendra Malik. End-to-end recovery of human shape and pose. In *IEEE Conference on Computer Vision and Pattern Recognition, CVPR 2018*.
- [22] Rawal Khrodkar, Shashank Tripathi, and Kris Kitani. Occluded human mesh recovery. In *IEEE/CVF Conference on Computer Vision and Pattern Recognition, CVPR 2022*.
- [23] Sena Kiciroglu, Helge Rhodin, Sudipta N. Sinha, Mathieu Salzmann, and Pascal Fua. Activemocap: Optimized viewpoint selection for active human motion capture. In *IEEE/CVF Conference on Computer Vision and Pattern Recognition, CVPR 2020*.
- [24] Imry Kissos, Lior Fritz, Matan Goldman, Omer Meir, Eduard Oks, and Mark Kliger. Beyond weak perspective for monocular 3d human pose estimation. In *European Conference on Computer Vision Workshops, ECCVW 2020*.
- [25] Muhammed Kocabas, Chun-Hao P. Huang, Otmar Hilliges, and Michael J. Black. PARE: part attention regressor for 3d human body estimation. In *IEEE/CVF International Conference on Computer Vision, ICCV 2021*.
- [26] Nikos Kolotouros, Georgios Pavlakos, Michael J. Black, and Kostas Daniilidis. Learning to reconstruct 3d human pose and shape via model-fitting in the loop. In *IEEE/CVF International Conference on Computer Vision, ICCV 2019*.
- [27] Nikos Kolotouros, Georgios Pavlakos, Dinesh Jayaraman, and Kostas Daniilidis. Probabilistic modeling for human mesh recovery. In *IEEE/CVF International Conference on Computer Vision, ICCV 2021*.
- [28] Chen Li and Gim Hee Lee. Generating multiple hypotheses for 3d human pose estimation with mixture density network. In *IEEE Conference on Computer Vision and Pattern Recognition, CVPR 2019*.
- [29] Kevin Lin, Lijuan Wang, and Zicheng Liu. End-to-end human pose and mesh reconstruction with transformers. In *IEEE Conference on Computer Vision and Pattern Recognition, CVPR 2021*.
- [30] Guanze Liu, Yu Rong, and Lu Sheng. VoteHMR: Occlusion-aware voting network for robust 3d human mesh recovery from partial point clouds. In *ACM Multimedia Conference, MM 2021*.
- [31] Matthew Loper, Naureen Mahmood, Javier Romero, Gerard Pons-Moll, and Michael J. Black. SMPL: a skinned multi-person linear model. *ACM Trans. Graph.*, 34(6):248:1–248:16, 2015.
- [32] Naureen Mahmood, Nima Ghorbani, Nikolaus F. Troje, Gerard Pons-Moll, and Michael J. Black. AMASS: archive of motion capture as surface shapes. In *IEEE/CVF International Conference on Computer Vision, ICCV 2019*.
- [33] Dushyant Mehta, Helge Rhodin, Dan Casas, Pascal Fua, Oleksandr Sotnychenko, Weipeng Xu, and Christian Theobalt. Monocular 3d human pose estimation in the wild using improved CNN supervision. In *International Conference on 3D Vision, 3DV 2017*.
- [34] Volodymyr Mnih, Koray Kavukcuoglu, David Silver, Alex Graves, Ioannis Antonoglou, Daan Wierstra, and Martin A. Riedmiller. Playing atari with deep reinforcement learning. *CoRR*, abs/1312.5602, 2013.
- [35] Soonchan Park and Jinah Park. Localizing human keypoints beyond the bounding box. In *IEEE/CVF International Conference on Computer Vision Workshops, ICCVW 2021*.
- [36] Georgios Pavlakos, Vasileios Choutas, Nima Ghorbani, Timo Bolkart, Ahmed A. A. Osman, Dimitrios Tzionas, and Michael J. Black. Expressive body capture: 3d hands, face, and body from a single image. In *IEEE Conference on Computer Vision and Pattern Recognition, CVPR 2019*.
- [37] Sida Peng, Yuanqing Zhang, Yinghao Xu, Qianqian Wang, Qing Shuai, Hujun Bao, and Xiaowei Zhou. Neural body: Implicit neural representations with structured latent codes for novel view synthesis of dynamic humans. In *IEEE Conference on Computer Vision and Pattern Recognition, CVPR 2021*.
- [38] Xi Peng, Zhiqiang Tang, Fei Yang, Rogério Schmidt Feris, and Dimitris N. Metaxas. Jointly optimize data augmentation and network training: Adversarial data augmentation in human pose estimation. In *IEEE/CVF Conference on Computer Vision and Pattern Recognition, CVPR 2018*.
- [39] Ke Sun, Bin Xiao, Dong Liu, and Jingdong Wang. Deep high-resolution representation learning for human pose estimation. In *IEEE Conference on Computer Vision and Pattern Recognition, CVPR 2019*.
- [40] Timo von Marcard, Roberto Henschel, Michael J. Black, Bodo Rosenhahn, and Gerard Pons-Moll. Recovering accurate 3d human pose in the wild using imus and a moving camera. In *European Conference on Computer Vision, ECCV 2018*.
- [41] Timo von Marcard, Bodo Rosenhahn, Michael J. Black, and Gerard Pons-Moll. Sparse inertial poser: Automatic 3d human pose estimation from sparse imus. *Comput. Graph. Forum*, 36(2):349–360, 2017.
- [42] Bastian Wandt and Bodo Rosenhahn. Repnet: Weakly supervised training of an adversarial reprojection network for 3d human pose estimation. In *IEEE Conference on Computer Vision and Pattern Recognition, CVPR 2019*.
- [43] Kangkan Wang, Jin Xie, Guofeng Zhang, Lei Liu, and Jian Yang. Sequential 3d human pose and shape estimation from point clouds. In

IEEE/CVF Conference on Computer Vision and Pattern Recognition, CVPR 2020.

- [44] Tom Wehrbein, Marco Rudolph, Bodo Rosenhahn, and Bastian Wandt. Probabilistic monocular 3d human pose estimation with normalizing flows. In *IEEE/CVF International Conference on Computer Vision, ICCV 2021*.
- [45] Shih-En Wei, Varun Ramakrishna, Takeo Kanade, and Yaser Sheikh. Convolutional pose machines. In *IEEE Conference on Computer Vision and Pattern Recognition, CVPR 2016*.
- [46] Bin Xiao, Haiping Wu, and Yichen Wei. Simple baselines for human pose estimation and tracking. In *European Conference on Computer Vision, ECCV 2018*.
- [47] Fu Xiong, Boshen Zhang, Yang Xiao, Zhiguo Cao, Taidong Yu, Joey Tianyi Zhou, and Junsong Yuan. A2J: anchor-to-joint regression network for 3d articulated pose estimation from a single depth image. In *IEEE/CVF International Conference on Computer Vision, ICCV 2019*.
- [48] Yuanlu Xu, Wenguan Wang, Tengyu Liu, Xiaobai Liu, Jianwen Xie, and Song-Chun Zhu. Monocular 3d pose estimation via pose grammar and data augmentation. *IEEE Trans. Pattern Anal. Mach. Intell.*, 44(10):6327–6344, 2022.
- [49] Takashi Yamamoto, Tamaki Nishino, Hideki Kajima, Mitsunori Ohta, and Koichi Ikeda. Human support robot (HSR). In *ACM Special Interest Group on Computer Graphics and Interactive Techniques Conference, SIGGRAPH 2018*.
- [50] Takashi Yamamoto, Koji Terada, Akiyoshi Ochiai, Fuminori Saito, Yoshiaki Asahara, and Kazuto Murase. Development of human support robot as the research platform of a domestic mobile manipulator. *ROBOMECH journal*, 6(1):1–15, 2019.
- [51] Jie Yang, Ailing Zeng, Shilong Liu, Feng Li, Ruimao Zhang, and Lei Zhang. Explicit box detection unifies end-to-end multi-person pose estimation. In *The Eleventh International Conference on Learning Representations, ICLR 2023*.
- [52] Ye Yuan, Umar Iqbal, Pavlo Molchanov, Kris Kitani, and Jan Kautz. GLAMR: global occlusion-aware human mesh recovery with dynamic cameras. In *IEEE/CVF Conference on Computer Vision and Pattern Recognition, CVPR 2022*.
- [53] Jianfeng Zhang, Xuecheng Nie, and Jiashi Feng. Inference stage optimization for cross-scenario 3d human pose estimation. In *Annual Conference on Neural Information Processing Systems, NeurIPS 2020*.
- [54] Jinlu Zhang, Zhigang Tu, Jianyu Yang, Yujin Chen, and Junsong Yuan. Mixste: Seq2seq mixed spatio-temporal encoder for 3d human pose estimation in video. In *IEEE/CVF Conference on Computer Vision and Pattern Recognition, CVPR 2022*.
- [55] Zhe Zhang, Chunyu Wang, Wenhui Qin, and Wenjun Zeng. Fusing wearable imus with multi-view images for human pose estimation: A geometric approach. In *IEEE/CVF Conference on Computer Vision and Pattern Recognition, CVPR 2020*.
- [56] Mingmin Zhao, Yingcheng Liu, Aniruddh Raghu, Hang Zhao, Tianhong Li, Antonio Torralba, and Dina Katabi. Through-wall human mesh recovery using radio signals. In *IEEE/CVF International Conference on Computer Vision, ICCV 2019*.
- [57] Mingmin Zhao, Yonglong Tian, Hang Zhao, Mohammad Abu Al-sheikh, Tianhong Li, Rumen Hristov, Zachary Kabelac, Dina Katabi, and Antonio Torralba. Rf-based 3d skeletons. In *Conference of the ACM Special Interest Group on Data Communication, SIGCOMM 2018*.
- [58] Tiancheng Zhi, Christoph Lassner, Tony Tung, Carsten Stoll, Srini-vasa G. Narasimhan, and Minh Vo. Texmesh: Reconstructing detailed human texture and geometry from RGB-D video. In *European Conference on Computer Vision, ECCV 2020*.
- [59] Lu Zhou, Yingying Chen, Yunze Gao, Jinqiao Wang, and Hanqing Lu. Occlusion-aware siamese network for human pose estimation. In *European Conference on Computer Vision, ECCV 2020*.